THE JOURNAL OF BIOLOGICAL CHEMISTRY
Vol. 279, No. 37, Issue of September 10, pp. 38803–38812, 2004
Printed in U.S.A.

Post-translational Modification of Rta of Epstein-Barr Virus by SUMO-1*

Received for publication, May 17, 2004, and in revised form, June 29, 2004
Published, JBC Papers in Press, June 30, 2004, DOI 10.1074/jbc.M405470200

Li-Kwan Chang‡, Yu-Hsiu Lee§, Tai-Shan Cheng‡, Yi-Ren Hong‡, Pei-Jung Lu¶, Janng J. Wang‖, Wen-Hung Wang§, Chung-Wen Kuo§, Steven S.-L. Li, and Shih-Tung Liu§‡‡**

*From the ‡Faculty of Biological Medicine and Environmental Biology and Graduate Institute of Biochemistry, Kaohsiung Medical University, 100, Shih-Chuan 1st Road, Kaohsiung 807, the §Molecular Genetics Laboratory, Department of Microbiology and Immunology, Chang Gung University, 259, Wen-Hua 1st Road, Kwei-Shan, Taoyuan 333, the ¶Department of Medical Education and Research, Veterans General Hospital, Kaohsiung, 386 Ta-Chung 1st Road, Kaohsiung 813, the ‖Institute of Biology and Anatomy, National Defense Medical School, 161, Section 6, Min-Chuang E. Road, Taipei 114, and the **Institute of Biomedical Sciences, National Sun Yat-Sen University, Kaohsiung 804, Taiwan*

Epstein-Barr virus (EBV) expresses an immediate-early protein, Rta, to activate the transcription of EBV lytic genes and the lytic cycle. This work identifies Ubc9 and PIAS1 as binding partners of Rta in a yeast two-hybrid screen. These bindings are verified by glutathione *S*-transferase pull-down assay, coimmunoprecipitation, and confocal microscopy. The interactions appear to cause Rta sumoylation, because not only can Rta be sumoylated *in vitro* but also sumoylated Rta can be detected in P3HR1 cells following lytic induction and in 293T cells after transfecting plasmids that express Rta and SUMO-1. Moreover, PIAS1 stimulates conjugation of SUMO-1 to Rta, thus acting as an E3 ligase. Furthermore, transfecting plasmids that express Ubc9, PIAS1, and SUMO-1 increases the capacity of Rta to transactivate the promoter that includes an Rta response element, indicating that the modification by SUMO-1 increases the transactivation activity of Rta. This study reveals that Rta is sumoylated at the Lys-19, Lys-213, and Lys-517 residues and that SUMO-1 conjugation at the Lys-19 residue is crucial for enhancing the transactivation activity of Rta. These results indicate that sumoylation of Rta may be important in EBV lytic activation.

Small ubiquitin-like modifiers (SUMOs)[1] are a group of proteins that conjugate a wide range of proteins in the cell (1–3). In human cells, three types of SUMO, *i.e.* SUMO-1, SUMO-2, and SUMO-3, have been identified (4–7). These SUMO molecules conjugate to their target proteins through an isopeptide bond formed between the C-terminal glycine residue of SUMO and a lysine residue in the substrate, frequently found at a conserved ψKXE motif; where ψ represents a hydrophobic amino acid residue, including Leu, Ile, Val, or Phe (8, 9). As is generally known, in a SUMO conjugation reaction, SUMO hydrolase first removes the four C-terminal amino acids of SUMO, exposing a glycine residue to facilitate SUMO conjugation. The SUMO molecule is then adenylated and covalently linked to a SUMO-activating E1 enzyme (10, 11). Subsequently, SUMO is transferred to the SUMO-conjugating E2 enzyme, Ubc9, which catalyzes the transfer of SUMO to its target proteins (12–15). The E3 ligase, which stimulates SUMO-1 conjugation to target proteins, has only recently been identified. Three proteins, including PIAS, RanBP2, and Pc2, are currently known to participate in the process of sumoylation (16–20). Sumoylation may influence protein functions in many ways. An important function of SUMO is to stabilize its target proteins by acting as an antagonist to ubiquitin-mediated proteolysis (21). For instance, SUMO modification blocks ubiquitination and destruction of IκB by the SCF(β-TrCP) E3 ubiquitin ligase complex (21), thus stabilizing the ability of IκB to inhibit NF-κB. SUMO modification is also known to influence protein localization. For example, SUMO-1 modification not only targets promyelocytic leukemia protein (PML) to discrete subnuclear structures called PML nuclear bodies (22) but also is necessary for RanGAP1 binding to a nuclear pore complex (23), which contains Ubc9 and RanBP2. Furthermore, both Ubc9 and RanBP2 are crucial for sumoylation, because Pichler *et al.* (17) and Zhang *et al.* (24) demonstrated that proteins are sumoylated on the cytoplasm side of nuclear membrane by Ubc9, and the sumoylated proteins are then transported into the nucleus by RanBP2 after sumoylation (17). Additionally, SUMO modification of Sp100 and Daxx targets these transcription factors into the PML nuclear bodies (25–27). As is generally known, the interphase nucleus is organized into distinct domains, including nuclear matrix and the chromatin structures of the chromosomes. PML nuclear bodies are essential domains of nuclear matrix (28), possibly accounting for why the activity of Sp100 and Daxx is activated after sumoylation. SUMO modification also regulates the DNA-binding activities of the heat shock transcription factors HSF1 and HSF2 (29, 30). On the other hand, sumoylation may actually inhibit transactivation activity of some transcription factors (31, 32). For example, SUMO modification inactivates the functions of Sp3 and changes its subnuclear localization (33, 34). Moreover, sumoylation influences the functions of many viral proteins. For instance,

* This work was supported by Medical Research Grant CMRP720-VI from Chang-Gung Memorial Hospital, National Health Research Institute Grant NHRI-EX91-8901SL, and National Council Grants NSC-91-2320-B-182-048, NSC-92-2311-B-037-002, and NSC-91-3112-B-110-001. The costs of publication of this article were defrayed in part by the payment of page charges. This article must therefore be hereby marked "*advertisement*" in accordance with 18 U.S.C. Section 1734 solely to indicate this fact.

‡‡ To whom correspondence should be addressed. Tel./Fax: 886-3-211-8292; E-mail: cgliu@mail.cgu.edu.tw.

[1] The abbreviations used are: SUMO, small ubiquitin-like modifier; E2, ubiquitin carrier protein ligase; E3, ubiquitin-protein isopeptide ligase; PML, promyelocytic leukemia protein; CMV, cytomegalovirus; EBV, Epstein-Barr virus; TPA, 12-*O*-tetradecanoylphorbol 13-acetate; TSA, trichostatin A; HA, hemagglutinin; GST, glutathione *S*-transferase; RRE, Rta response element; DTT, dithiothreitol; PBS, phosphate-buffered saline; MALDI-TOF, matrix-assisted laser desorption ionization time-of-flight; NEM, *N*-ethylmaleimide; TRITC, tetramethyl rhodamine isothiocyanate.

SUMO conjugation of papillomavirus E1 increases its ability to enhance viral DNA replication (35); SUMO-1 modification also increases the transactivation activity of human cytomegalovirus (CMV) IE2 (36, 51). Although CMV IE1/IE72 is modified by SUMO-1, exactly how such modification affects the functions of IE1/IE72 remains unknown (37, 61, 62).

Epstein-Barr virus (EBV) is normally maintained under latent conditions in B lymphocytes. However, EBV must enter a lytic phase to proliferate. During the immediate-early stage of the lytic cycle, the virus expresses two immediate-early proteins, *i.e.* Rta and Zta, to activate the viral early genes and the lytic cascade (38–42). Adamson and Kenney (43) demonstrated that Zta is modified by SUMO-1. Such modification may compete with PML for limited amounts of SUMO-1 in the nucleus, thus preventing the formation of PML nuclear bodies and resulting in a dispersion of PML nuclear bodies in the nucleus (43). In addition, the EBNA-3C protein of EBV is sumoylated, which appears to be crucial for activating the BNLF1 promoter by EBNA-3C (44, 45). This investigation demonstrates that Rta is sumoylated by SUMO-1 and, in doing so, enhances the transactivation activity of Rta.

EXPERIMENTAL PROCEDURES

Cell Lines and EBV Lytic Induction—P3HR1, Jurkat, and EBV-negative Akata cells were cultured in RPMI 1640 medium containing 10% fetal calf serum. 293T cells were cultured in Dulbecco's modified Eagle's medium supplemented with 10% fetal calf serum. To activate the EBV lytic cycle, P3HR1 cells were treated with 12-*O*-tetradecanoylphorbol 13-acetate (TPA) and sodium butyrate or trichostatin A (TSA) according to a method described elsewhere (38, 46, 47).

Plasmids—Plasmid pCMV-R contains BRLF1 transcribed from the CMV immediate-early promoter (39). Plasmid pCMV-3 is identical to pCMV-R except without BRLF1. Plasmids pcDNA-Ubc9 and pGEX-Ubc9, which express HA-tagged Ubc9 and GST-Ubc9, respectively, were provided by Van G. Wilson (35). Plasmid pCR-SUMO-1, which encodes FLAG-tagged SUMO-1, was constructed by inserting a PCR-amplified SUMO-1 DNA fragment into pCR3.1 (Invitrogen). Plasmid pGEX-4T1, which expresses GST, was purchased from Amersham Biosciences. Plasmid pET-SUMO-1, which expresses His-tagged SUMO-1 in *Escherichia coli* BL21(DE3), was constructed by inserting a SUMO-1 DNA fragment into the EcoRI and XhoI sites of pET-28a (Novagen, Madison, WI). Plasmids pCMV-PIAS1 and pGEX-PIAS1 were provided by Stefan Müller (48). Double-stranded DNA (5′-CCCAAGCTTCGGCTGACATGAATTCCTGGTCTTTTATCATGTCCCTCTATCATGGCGCAGACCCCGGGGGA), which contains an Rta response element (RRE) from the BMLF1 promoter and a TATA sequence, was synthesized and inserted into the HindIII and SmaI sites, upstream of a firefly luciferase gene (*luc*), in pGL2-Basic (Promega) to generate pRRE. To construct a plasmid (pET-Rta) expressing Rta in *E. coli* BL21(DE3), BRLF1 was amplified by PCR, using primers GST-5R (5′-CCGGAATTCCGGAGGCCTAAAAAGGATGGC) and GST-3R. The fragment was then inserted into the EcoRI and SalI sites in pET-32a(+) (Novagen). Plasmid pGEX-SUMO-1 (23), obtained from Frauke Melchior, encodes a GST-SUMO-1 fusion protein that lacks the four C-terminal amino acids of SUMO-1. A DNA fragment encoding Ubc9 was amplified by PCR, using U1 (5′-CGGGATCCACATGTCGGGGATCGCCCTCAGC) and U2 (5′-ACGCGTCGACTTATGAGGGCGCAAACTTCTTGGC) as primers and a human testis cDNA library as template. The fragment was digested with BamHI and SalI and inserted into the BamHI-SalI sites in pACT2 to generate pACT-Ubc9. Plasmid pACT-PIAS1 was isolated from a human testis cDNA library constructed in pACT2 (Clontech, Palo Alto, CA). A plasmid that expresses full-length Rta tagged with an HA sequence at the N terminus (HA-Rta) was constructed by inserting a PCR-amplified BRLF1 fragment into pcDNA3-HA at the EcoRI and SalI sites. Plasmids that expressed deleted HA-Rta were constructed in the same way. These Rta deletion mutants include RN122, RN190, and RN347, as well as RC351, which lacked the regions from amino acids 123 to 605, 191 to 605, and 348 to 605, and 1 to 254, respectively. Meanwhile, mutant R255/415 included the region between amino acids 255 and 415 of Rta. Lysine residues at amino acid positions 19, 213, and 517 on HA-Rta were mutagenized following a PCR mutagenesis method of Ho (49).

Yeast Two-hybrid Screen—To construct a bait plasmid for yeast two-hybrid screening, BRLF1 was amplified by PCR, using R1 (5′-CATGCCATGGCGATGAGGCCTAAAAAGGATGGC) and R2 (5′-CATGCCATGGCTAAAATAAGCTGGTGTCAAAA) as primers and pCMV-R as template. The fragment was digested with NcoI and inserted into the NcoI site of pAS2-1 (Clontech). The orientation of the insert was subsequently verified by DNA sequencing. The plasmid was then digested with BamHI to remove the 3′ region of BRLF1 to generate pR476, which encodes the Gal4 DNA-binding domain fused with the N-terminal 476 amino acids of Rta. A human testis cDNA library constructed in pACT2 (Clontech) was screened by cotransforming the bait (pR476) and the library plasmids into yeast strain, YRG-2 (Stratagene, La Jolla, CA). Positive clones were selected based on their ability to grow on Trp, Leu, and His dropout media supplemented with 3-aminotriazole and their blue colony color in β-galactosidase filter assay. These phenotypes were further confirmed in yeast strain Y190. β-Galactosidase activity was determined in Z buffer (150 mM phosphate buffer, pH 7.0, 10 mM KCl, and 1 mM $MgSO_4$) containing 4 mg/ml *O*-nitrophenyl-β-D-galactopyranoside. Reactions were performed at 30 °C and stopped by adding 250 mM sodium carbonate. Enzyme activity was determined by measuring absorbance at 420 nm with a spectrophotometer (Model U2000, Hitachi, Japan).

Purification of GST Fusion Proteins—To purify GST-Ubc9, 1 liter of *E. coli* BL21(DE3) (pGEX-Ubc9) was cultured to mid-log phase in 1 liter of LB medium. isopropyl-1-thio-β-D-galactopyranoside was then added to the medium to a final concentration of 1 mM. Cells were harvested 4 h after the treatment, suspended in ice-cold buffer A (50 mM Tris-HCl, pH 8.0, 500 mM NaCl, 1 mM DTT, 1 mM 4-(2-aminoethyl)benzenesulfonyl fluoride, and 1 mM leupeptin), and homogenized by sonication for 1 min. Cell lysate was then centrifuged at 6000 × *g* for 10 min at 4 °C. The supernatant was applied to a column containing 1 ml of glutathione-agarose beads (Amersham Biosciences). The column was washed with ten column volumes of buffer A. GST-Ubc9 was finally eluted from the column by adding buffer A containing 20 mM glutathione. The eluted GST-Ubc9 was dialyzed for 16 h against a dialysis buffer containing 50 mM Tris-HCl, pH 7.6, 100 mM NaCl, and 1 mM DTT. Dialyzed GST-Ubc9 was concentrated to 8 mg/ml with Centricon-100 (Millipore, Bedford, MA) and stored at −80 °C until use. GST, GST-PIAS1, and GST-SUMO-1 were purified by the same method. His-tagged SUMO-1 and His-tagged Rta expressed by *E. coli* BL21(DE3)(pET-SUMO-1) and *E. coli* BL21(DE3)(pET-Rta), respectively, were purified by a similar method, except that the protein was purified with a nickel-nitrilotriacetic acid column, eluted with 200 mM imidazole, and concentrated to a final concentration of 20 mg/ml.

GST-pull-down Assay—GST, GST-Ubc9, GST-SUMO-1, or GST-PIAS1, at a concentration of 40 ng/ml in 500 μl of NETN buffer (20 mM Tris-HCl, pH 8.0, 100 mM NaCl, 1 mM EDTA, 0.5% Nonidet P-40) containing 10 μg/ml each of leupeptin, aprotinin, and 4-(2-aminoethyl)-benzenesulfonyl fluoride, was added to 30 μl of glutathione-Sepharose 4B beads (Amersham Biosciences). The mixture was incubated under shaking for 1 h at 4 °C. The beads were washed three times with NETN buffer and added to the lysate (300 μl) prepared from *E. coli* BL21(DE3)(pET-Rta), P3HR1 cells, or 293T cells transfected with a plasmid that expresses Rta or its deletion derivatives. The reaction mixture was incubated on ice for 1 h. The beads were subsequently washed with NETN buffer. An equal volume of 2× electrophoresis sample buffer was added to the mixture, and proteins were extracted from the beads by heating at 95 °C for 5 min. Proteins were finally separated by SDS-polyacrylamide gel electrophoresis (50).

Immunoblot Analysis—Proteins resolved by SDS-polyacrylamide gel were electrotransferred to a Hybond C membrane (Amersham Biosciences) at 90 V for 1 h and probed with the appropriate antibodies. SuperSignal West Pico chemiluminescent substrate (Pierce) was used to visualize the proteins on the membrane.

Immunoprecipitation—P3HR1 cells (1×10^7) transfected with pCMV-R, pcDNA-Ubc9, pCMV-PIAS1, or pCR-SUMO-1 were washed with phosphate-buffered saline (PBS). The lysate was prepared by adding 1 ml of radioimmune precipitation assay buffer (50 mM Tris-HCl, pH 7.8, 150 mM NaCl, 5 mM EDTA, 0.5% Triton X-100, 0.5% Nonidet P-40, 0.1% deoxycholate, and 10 μg/ml each of leupeptin, aprotinin, and 4-(2-aminoethyl)benzenesulfonyl fluoride) to the cells. Then the lysate was centrifuged with a microcentrifuge at 10,000 × *g* for 20 min. The supernatant was added with anti-Rta (1:500 dilution) (Argene, Varilhes, France) or anti-HA (1:500 dilution) (Roche Applied Science) antibody at 4 °C for 1 h. Protein-A/G-agarose beads (30 μl) (Oncogene, Boston, MA) were added to the lysate, and the mixture was incubated under shaking for 1 h at 4 °C. The beads were finally collected by centrifugation and washed three times with radioimmune precipitation assay buffer. Proteins binding to the beads were eluted by adding 20 μl of 2× electrophoresis sample buffer and analyzed by immunoblotting with anti-HA antibody. For MALDI-

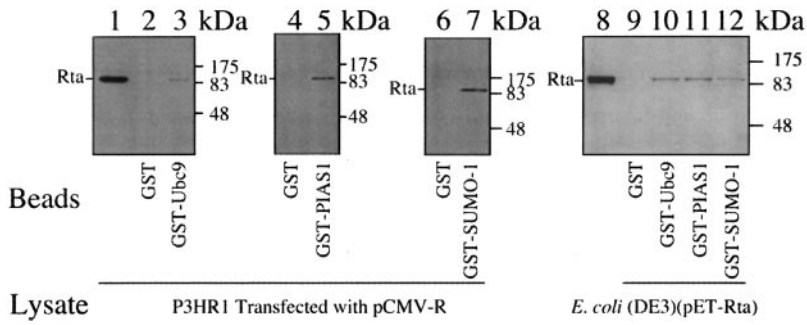

FIG. 1. **GST-pull-down assays.** Lysate prepared from P3HR1 cells transfected with pCMV-R (*lanes 1–7*) or from *E. coli* BL21(DE3)(pET-Rta) (*lanes 8–12*) was added to GST (*lanes 2*, *4*, *6*, and *9*), GST-Ubc9- (*lanes 3* and *10*), GST-PIAS1- (*lanes 5* and *11*), and GST-SUMO-1- (*lanes 7* and *12*) glutathione-Sepharose beads. *Lanes 1* and *8* were loaded with cell lysate. Proteins on the beads were finally analyzed by immunoblot analysis with anti-Rta antibody. Beads: GST or GST fusion protein binding to glutathione-Sepharose beads.

TOF mass spectrometry analysis, Rta was immunoprecipitated from the lysate prepared from 6×10^7 P3HR1 cells transfected with 120 μg of pCMV-R. Immunoprecipitation was performed in four tubes. After immunoprecipitation, proteins were pooled and separated by SDS-polyacrylamide gel electrophoresis. To detect sumoylated Rta after transfection, cells (1×10^7) were lysed according to a method described elsewhere (51). To examine Rta sumoylation in cell lysate after lytic induction, 1×10^7 of P3HR1 cells were treated with 100 nM TSA for 24 h before immunoprecipitation.

MALDI-TOF Mass Spectrometry Analysis of Rta—An 88-kDa protein immunoprecipitated by anti-Rta antibody was excised from an SDS-polyacrylamide gel and analyzed by MALDI-TOF mass spectrometry analysis by Accelerating Biodigital Era Inc. (Taipei, Taiwan).

In Vitro SUMO Conjugation—Bacterially expressed Rta, SUMO-1 lacking the four C-terminal amino acids, GST-PIAS1, and SUMO-activating E1 enzyme (LAE Biotechnology Co., Taipei, Taiwan) were used to examine Rta sumoylation *in vitro*. Each SUMO conjugation reaction (16 μl) contained 1 μg of purified Rta, 500 ng each of GST-Ubc9 and SUMO-1, 15 ng of SUMO-activating E1 enzyme, and 4 μl of a buffer containing 200 mM Tris-HCl, pH 7.8, 20 mM $MgCl_2$, 20 mM ATP, 4 mM DTT, and 800 μM NEM. Meanwhile, one-tenth of the amount of E1 and E2 was used to study the enhancement of Rta sumoylation by PIAS1. Reaction mixtures were incubated at 37 °C for 1 h. After incubation, 16 μl of 2× electrophoresis sample buffer was added to the reaction mixtures, which were then heated at 95 °C for 5 min. Proteins in the mixtures were immediately separated by SDS-polyacrylamide gel electrophoresis. Rta was then detected by immunoblotting with anti-Rta antibody.

Transient Transfection Assay—Plasmids were purified from *E. coli* by CsCl-gradient centrifugation (50). Plasmids (10 μg) were transfected into EBV-negative Akata and Jurkat cells by electroporation with a Bio-Rad Gene-Pulser electroporator (39). A luciferase assay was performed, using a luminometer (model LB593, Berthod, Bad Wildbad, Germany), according to a method described elsewhere (39). Each transfection experiment was performed three times, and each sample in the experiment was prepared in duplicate.

Immunofluorescence Analysis—P3HR1 cells were treated with 30 ng/ml TPA and 3 mM sodium butyrate for 24 h to induce the expression of Rta. Cells were then harvested by centrifugation, plated on poly-L-lysine (Sigma)-coated coverslips, and fixed with 4% paraformaldehyde in PBS for 30 min. The cells were then incubated for 1 h with anti-Rta monoclonal antibody, goat anti-Ubc9 polyclonal antibody, goat anti-PIAS1 polyclonal antibody (Santa Cruz Biotechnology Inc.), or rabbit anti-SUMO-1 polyclonal antibody (Santa Cruz Biotechnology Inc.) and then treated with fluorescein isothiocyanate-conjugated goat anti-mouse IgG polyclonal antibody (KPL Inc., Gaithersburg, MD), fluorescein isothiocyanate-conjugated rabbit anti-mouse IgG polyclonal antibody (DAKO, Glostrup, Denmark), TRITC-conjugated rabbit anti-goat IgG polyclonal antibody (KPL, Inc.), or TRITC-conjugated goat anti-rabbit IgG polyclonal antibody (KPL Inc.). Finally, cells were washed with PBS, mounted in CITIFLOUR (Agar Inc., Essex, England), and examined with a Model LSM510 Zeiss confocal laser scanning microscope (Oberkochen, Germany).

RESULTS

Identification of Ubc9 and PIAS1 as Rta-binding Proteins—Yeast two-hybrid screening was performed in strain YRG2, with a bait plasmid, pR476, which expresses a protein (RN476) that contains the Gal4 DNA-binding domain fused with the N-terminal 476 amino acids of Rta. RN476 lacks an intact transactivation domain, preventing it from activating the reporter genes and changing the phenotypes of yeast strain YRG2. Strain YRG2(pR476) was subsequently transformed with a human testes cDNA library constructed in pACT2 to screen the proteins that interact with Rta. This study screened $\sim 6 \times 10^5$ transformants and identified 24 plasmids that encode seven cellular proteins. Sequencing analysis revealed that, among the 24 clones, cDNA that encodes Ubc9 and PIAS1 was isolated seven times and twice, respectively. β-Galactosidase assay revealed that yeast strain Y190(pR476) transformed with a yeast two-hybrid cloning vector, pACT2, produced 25 units of β-galactosidase activity. However, this value increased to 1190 or 810 units when the strain was transformed with pACT-Ubc9 or pACT-PIAS1, respectively, indicating that RN476 interacts with Ubc9, and PIAS1.

Binding of Rta to Ubc9, PIAS1, and SUMO-1 in Vitro—GST fusion pull-down assays were performed with bacterially expressed GST-Ubc9 and GST-PIAS1, respectively, to investigate whether Rta interacts with Ubc9 and PIAS1 in a context other than in yeast. Furthermore, because interaction between Rta and Ubc9 or PIAS1 in yeasts implies that Rta is conjugated by SUMO-1, this study also investigated whether Rta interacted with SUMO-1. GST or GST-Ubc9 bound to glutathione-Sepharose beads was added to the lysate prepared from P3HR1 cells transfected with pCMV-R (Fig. 1, *lanes 2* and *3*). After extensive washing, proteins bound to the beads were precipitated and analyzed by immunoblotting with anti-Rta antibody. Results indicated that Rta in the lysate (Fig. 1, *lane 1*) was retained by GST-Ubc9-glutathione-Sepharose beads (Fig. 1, *lane 3*) but was not retained by GST-glutathione-Sepharose beads (Fig. 1, *lane 2*). A similar study also revealed that His-tagged Rta expressed by *E. coli* (Fig. 1, *lane 8*) was retained by GST-Ubc9- (Fig. 1, *lane 10*) but not by GST-glutathione-Sepharose beads (Fig. 1, *lane 9*), confirming the interaction between Rta and Ubc9. Meanwhile, using GST-PIAS1 and GST-SUMO-1 also produced similar results; *i.e.* Rta in P3HR1 lysate or in *E. coli* lysate was retained by GST-PIAS1- (Fig. 1, *lanes 5* and *11*) and GST-SUMO-1-glutathione-Sepharose beads (Fig. 1, *lanes 7* and *12*) but not retained by GST-glutathione-Sepharose beads (Fig. 1, *lanes 4*, *6*, and *9*), indicating that Rta interacts with PIAS1 and SUMO-1.

Determination of the Domains in Rta That Interact with Ubc9 and PIAS1—Plasmids that express deleted Rta (Fig. 2*A*) were transfected into 293T cells. GST-Ubc9- or GST-PIAS1-glutatione-Sepharose beads were subsequently added to cell lysate to elucidate whether the beads pulled down the deletion derivatives of Rta. Meanwhile, immunoblot analysis was conducted with anti-HA antibody to verify the expression of Rta by

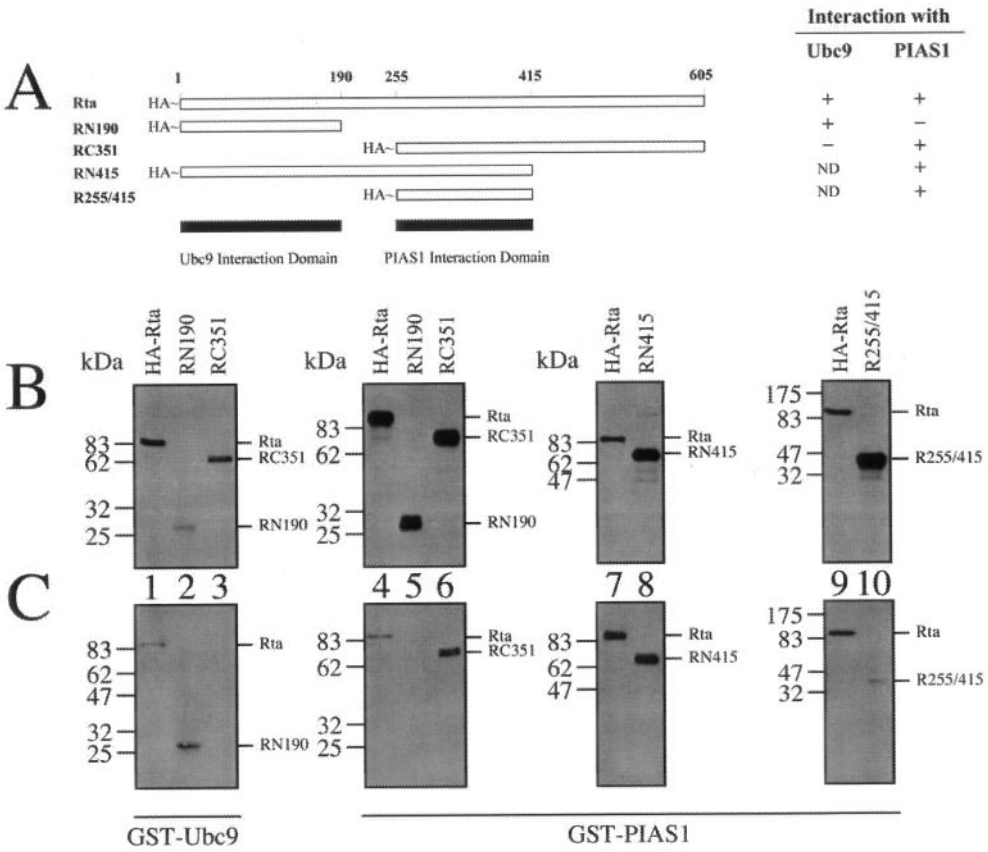

FIG. 2. **Delineation of the regions in Rta that interact with Ubc9 and PIAS1.** Plasmids that express HA-tagged Rta (*HA-Rta*) and its deletion derivatives (*A*) were transfected into 293T cells. Proteins in the lysate were detected by immunoblot analysis with anti-HA antibody (*B*). GST-Ubc9- and GST-PIAS1-glutathione-Separose beads were subsequently added to the lysate to pull down Rta and its deletion mutants (*C*). *ND*, not done.

the cells (Fig. 2*B*). Immunoblot analysis revealed HA-Rta was expressed by the cells (Fig. 2*B*, *lanes 1*, *4*, *7*, and *9*) and was retained by GST-Ubc9- (Fig. 2*C*, *lane 1*) and GST-PIAS1-glutathione-Sepharose beads (Fig. 2*C*, *lanes 4*, *7*, and *9*). On the other hand, GST-Ubc9-glutathione-Sepharose beads did not pull down HA-Rta that lacks the N-terminal 254 amino acids (RC351) (Fig. 2*C*, *lane 3*), indicating that the Ubc9-binding site is within the N-terminal 254-amino acid region (Fig. 2*A*). This finding was also supported by the fact that the GST-Ubc9-glutathione-Sepharose beads (Fig. 2*C*, *lane 2*) retained a peptide that contains an HA tag fused to the N-terminal 190 amino acids of Rta (RN190), indicating that Ubc9 binds to the N-terminal 190-amino acid region in Rta. A similar experiment was also performed to delineate the region that interacts with PIAS1. The results showed that GST-PIAS1-glutathione-Sepharose beads did not retain RN190 (Fig. 2*C*, *lane 5*). However, the beads retain a peptide that contained the N-terminal 415 amino acids of Rta (RN415) fused with an HA tag (Fig. 2*C*, *lane 8*), indicating that the region between amino acid 191 and 415 interacts with PIAS1 (Fig. 2*A*). Furthermore, GST-PIAS1-glutathione-Sepharose beads retained RC351 (Fig. 2*C*, *lane 6*). The retention of RN415 and RC351 suggested that the region between amino acids 255 and 415 in Rta contains a PIAS1-binding site (Fig. 2*A*). Finally, GST-PIAS1 retained a peptide that contains the sequence from amino acids 255 to 415 in Rta (Fig. 2*C*, *lane 10*), verifying the binding of this region to PAIS1.

Coimmunoprecipitation of Rta and Ubc9 or PIAS1—293T cells were cotransfected with plasmids that express Rta (pCMV-R) and HA-tagged Ubc9 (pcDNA-Ubc9) (Fig. 3*A*), and lysate was prepared 24 h after transfection to investigate whether Rta interacts with Ubc9 *in vivo*. Rta in the lysate was subsequently detected by immunoblot analysis with anti-Rta antibody (Fig. 3*A*, *lane 1*). Meanwhile, Rta was immunoprecipitated by anti-HA antibody and anti-Rta antibody bound to protein-A/G-agarose beads (Fig. 3*A*, *lanes 3* and *4*). However, Rta was undetected when no anti-Rta antibody or anti-HA antibody was added to the immunoprecipitation reaction (Fig. 3*A*, *lane 2*). Anti-HA antibody (Fig. 3*A*, *lane 8*) and anti-Rta antibody (Fig. 3*A*, *lane 7*) bound to protein-A/G-agarose beads also immunoprecipitated HA-tagged Ubc9 (Fig. 3*A*, *lanes 7* and *8*). Ubc9 was undetected, however, when no antibodies were added (Fig. 3*A*, *lane 6*). Additionally, similar experiments that involved cotransfection of pCMV-R and a plasmid that expresses HA-tagged PIAS1 (pCMV-PIAS1) also showed the binding of Rta to PIAS1. Rta and PIAS1 were coimmunoprecipitated by anti-HA antibody (Fig. 3*B*, *lane 3*) and anti-Rta antibody (Fig. 3*B*, *lane 7*), respectively. Notably, bands smaller than that of PIAS1 were observed in the immunoblot (Fig. 3*B*, *lanes 7* and *8*), which is attributed to overexposure of the blot to an x-ray film. Furthermore, neither anti-HA nor anti-Rta antibody immunoprecipitated Rta, Ubc9, and PIAS1 from the lysate prepared from the cells that were transfected with an empty vector (data not shown), indicating that the antibodies did not nonspecifically detect the proteins.

Subcellular Localization of Rta—To investigate the localization of Rta, P3HR1 cells were treated with TPA and sodium butyrate to induce Rta expression. Immunofluorescence analyses with a confocal microscope revealed that, although distributed evenly in the cytoplasm, Rta aggregated as *dots* in the nucleus (Fig. 4, *A*, *D*, and *G*). On the other hand, Rta was undetected if the cells were not treated with TPA and sodium butyrate (Fig. 4*J*). Ubc9 was present evenly and more abun-

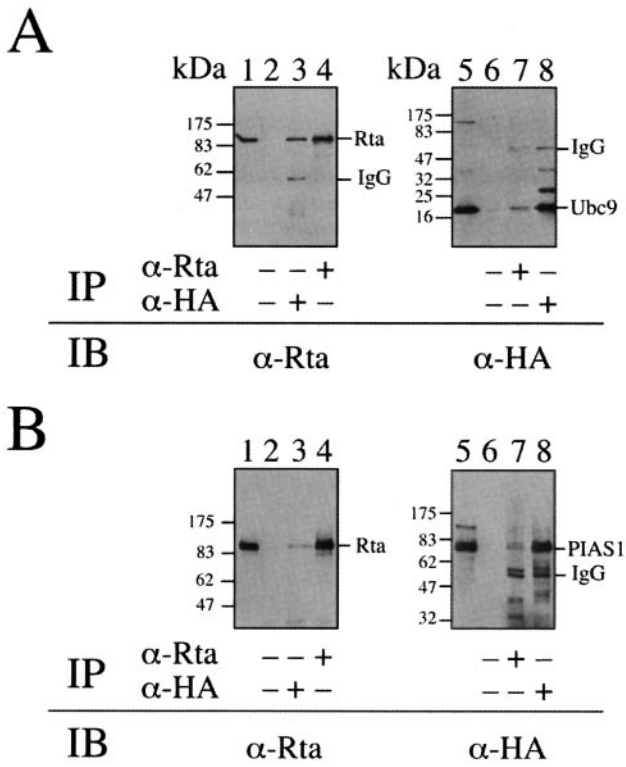

FIG. 3. **Binding of Rta to Ubc9 and PIAS1 *in vivo*.** 293T cells were cotransfected with pCMV-R and pcDNA-Ubc9 (*A*) or pCMV-PIAS1 (*B*). Lysate was subsequently prepared from the cells (*panels A* and *B*, *lanes 1* and *5*), and coimmunoprecipitation was performed with anti-Rta antibody (*panels A* and *B*, *lanes 4* and *7*) and anti-HA antibody (*panels A* and *B*, *lanes 3* and *8*). Immunoprecipitation (*IP*) was also performed with protein-A/G-agarose beads but without antibody (*panels A* and *B*, *lanes 2* and *6*). Immunoblotting (*IB*) was performed using anti-Rta antibody (*panels A* and *B*, *lanes 1–4*) and anti-HA antibody (*panels A* and *B*, *lanes 5–8*).

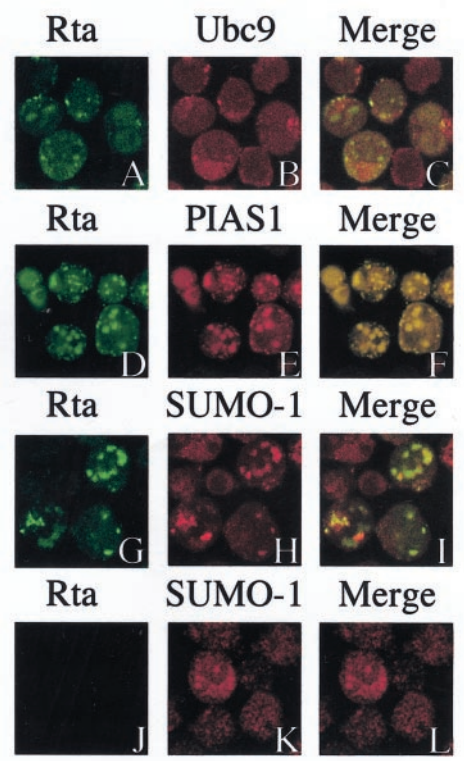

FIG. 4. **Indirect immunofluorescence analysis.** P3HR1 cells (*A–I*) were treated with TPA and sodium butyrate to induce the expression of Rta. Cells untreated with TPA and sodium butyrate are presented in *panels J–L*. Cells were incubated with monoclonal anti-Rta antibody (*A*, *D*, *G*, and *J*), goat anti-Ubc9 polyclonal antibody (*B*), goat anti-PIAS1 polyclonal antibody (*E*), and rabbit anti-SUMO-1 monoclonal antibody (*H* and *K*). Finally, cells were examined with a Model LSM510 Zeiss confocal laser scanning microscope. *C*, *F*, *I*, and *L* are merged images.

dantly in the cytoplasm than in the nucleus (Fig. 4*B*). A merged picture revealed that Ubc9 colocalized with Rta on the nuclear membrane (Fig. 4*C*). Meanwhile, PIAS1 colocalized with Rta on the nuclear membrane and in the nucleus (Fig. 4*F*). Similar to Ubc9, SUMO-1 was present in both the cytoplasm and nucleus (Fig. 4*H*) but colocalized with Rta in the nucleus as *large dots* (Fig. 4*I*). As expected, colocalization between Rta and SUMO-1 was not observed if the cells were not treated with TPA and sodium butyrate (Fig. 4*L*).

Immunoblot and MALDI-TOF Mass Spectrometry Analysis of Rta—Rta has 605 amino acids with an estimated molecular mass of 66 kDa. However, the migration pattern of Rta in an SDS-polyacrylamide gel is inconsistent with the predicted mass of the protein and typically migrates to a position higher than 66 kDa to the position of 88 kDa (Fig. 1, *lane 1*) (52). To demonstrate that the 88-kDa protein is Rta, in this study, we immunoprecipitated and separated Rta by SDS-polyacrylamide gel electrophoresis. The 88-kDa band was subsequently excised and digested with trypsin. MALDI-TOF mass spectrometry analysis of the digested protein revealed six peptides with a molecular mass consistent with the mass of peptide segments of Rta between amino acids 3–18, 63–77, 104–121, 242–262, 282–306, and 381–390, confirming that the 88-kDa protein is Rta.

Modification of Rta by SUMO-1 in Vitro and Enhancement of Rta Sumoylation by PIAS1—An *in vitro* sumoylation study, using purified Rta, SUMO-activating E1 enzyme, GST-Ubc9 (E2), and SUMO-1 lacking the four C-terminal amino acid residues, was performed to determine whether Rta is modified by SUMO-1. After incubation for 1 h at 37 °C, proteins in the reaction mixtures were analyzed by immunoblot analysis with anti-Rta antibody. In the reaction that contained SUMO-activating E1 enzyme, GST-Ubc9, and SUMO-1, proteins with a molecular mass larger than that of Rta were detected, suggesting that Rta is conjugated by SUMO-1 (Fig. 5*A*, *lane 3*). However, these bands were undetected if SUMO-activating E1 enzyme, GST-Ubc9, or SUMO-1 was not added to the reaction mixture (Fig. 5*A*, *lanes 2* and *4–7*), indicating that SUMO-activating E1 enzyme, GST-Ubc9, and SUMO-1 are necessary for Rta sumoylation *in vitro*. Notably, Rta was conjugated by SUMO-1 *in vitro* without PIAS1 (Fig. 5*A*, *lane 3*). A similar finding was observed for the *in vitro* sumoylation of p53 (53), suggesting that SUMO conjugation *in vitro* may not depend on PIAS1. On the other hand, PIAS1 appeared to enhance Rta sumoylation, because Rta sumoylation did not occur when the amount of SUMO-activating E1 enzyme and GST-Ubc9 was reduced 90% unless at least 160 ng of GST-PIAS1 was added to the reaction mixture (Fig. 5*B*, *lanes 4–6*). Additionally, the instability of Rta expressed in *E. coli* caused bands smaller than that of Rta to be frequently detected by anti-Rta antibody when an immunoblot was overexposed to an x-ray film (Fig. 5*B*, *lanes 1–6*). P3HR1 cells also were transfected with pCMV-R; sumoylated Rta was hardly detectable in the cell lysate (Fig. 5*C*, *lane 1*) unless the cells were also cotransfected with pCMV-PIAS1 (Fig. 5*C*, *lane 2*), further indicating that PIAS1 enhances Rta sumoylation. In this particular study (Fig. 5*C*, *lanes 1* and *2*), SDS and NEM were purposely omitted from the lysis buffer, which resulted in rapid de-sumoylation of Rta during cell lysis, explaining why sumoylated Rta was undetected in the lysate by immunoblotting (Fig. 5*C*, *lane 1*).

Modification of Rta by SUMO-1 in Vivo—After demonstrat-

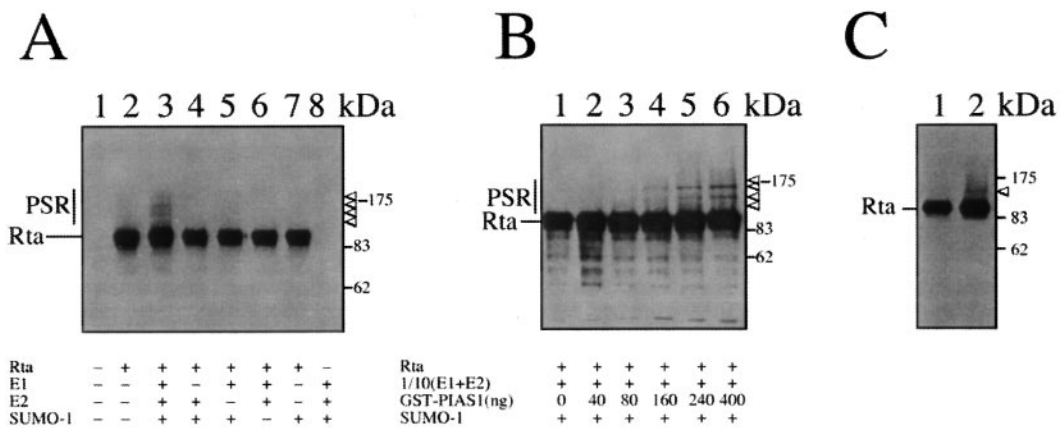

FIG. 5. **Modification of Rta by SUMO-1 *in vitro* and enhancement of Rta sumoylation by PIAS1.** *A*, conjugation of Rta by SUMO-1 was analyzed *in vitro* with purified Rta, SUMO E1, GST-Ubc9 (*E2*), and SUMO-1. *B*, the enhancement by PIAS1 of Rta sumoylation was studied in reaction mixtures that contained PIAS1 and one-tenth the amount of E1 and E2. *C*, Rta in the reaction mixtures was analyzed by immunoblot analysis with anti-Rta antibody. Furthermore, P3HR1 cells were transfected with pCMV-R (*lane 1*) or cotransfected with pCMV-R and pCMV-PIAS1 (*lane 2*). Rta in the lysate was analyzed with anti-Rta antibody to demonstrate the enhancement effect of PIAS1 on Rta sumoylation. *Triangles* (*A* and *B*: 125 kDa, 140 kDa, 160 kDa, 180 kDa; *C*: 140 kDa) refer to sumoylated Rta. *PSR*, polysumoylated Rta.

ing that Rta is sumoylated *in vitro*, this work further investigated whether Rta is modified by SUMO-1 *in vivo*. In the lysate prepared from P3HR1 cells treated with TSA, anti-Rta antibody detected two bands at the 140- and 160-kDa positions and two bands above 175 kDa (Fig. 6*A*, *lane 1*). These bands were also detectable by probing the immunoblot with anti-SUMO-1 antibody (Fig. 6*A*, *lane 2*). Because the amount of Rta expressed after TSA treatment was low (Fig. 6*A*, *lane 1*), this study further transfected P3HR1 cells with pCMV-R to achieve a high level expression of Rta. Under such conditions, an Rta band and a 140-kDa band were detectable by immunoblot analysis with anti-Rta antibody (Fig. 6*B*, *lane 2*). An immunoprecipitation study also showed that the 140-kDa protein was immunoprecipitated and detected using anti-Rta antibody (Fig. 6*B*, *lane 5*). Meanwhile, cotransfecting the cells with pCMV-R and pCR-SUMO-1 resulted in the detection of not only the 140-kDa but also a 160-kDa band (Fig. 6*B*, *lane 1*). These bands were also detected following immunoprecipitation and immunoblotting with anti-Rta antibody (Fig. 6*B*, *lane 4*). As expected, these proteins were undetected if the cells were not transfected with pCMV-R (Fig. 6*B*, *lanes 3* and *6*). Meanwhile, the 140-kDa protein was immunoprecipitated using anti-Rta antibody and detected by immunoblotting with anti-SUMO-1 antibody (Fig. 6*C*, *lane 2*), indicating that this 140-kDa protein is SUMO-1-conjugated Rta. Furthermore, a 140-kDa, a 160-kDa, and a 200-kDa band were detected with anti-SUMO-1 antibody when the cells were cotransfected with pCMV-R and pCR-SUMO-1 (Fig. 6*C*, *lane 1*), indicating that Rta is indeed conjugated by SUMO-1. However, these proteins could not be detected by anti-SUMO-1 antibody when the cells were not transfected with pCMV-R (Fig. 6*C*, *lane 3*). SUMO-1 expressed from pCR-SUMO-1 has a FLAG tag, so this investigation also immunoprecipitated proteins from cell lysate with anti-FLAG antibody (Fig. 6*D*, *lanes 1–3*). In the lysate prepared from cells transfected with only pCMV-R, a band above 83 kDa was detected with anti-Rta antibody (Fig. 6*D*, *lane 2*). However, this band is unrelated to Rta, because the protein is larger than Rta and was detected by anti-FLAG antibody even when the cells were not transfected with pCMV-R (Fig. 6*D*, *lane 3*). However, at least three bands, 140 kDa, 160 kDa, and 200 kDa, were detected by anti-Rta antibody when the proteins in the lysate prepared from the cells transfected with pCMV-R and pCR-SUMO-1 were immunoprecipitated using anti-FLAG antibody (Fig. 6*D*, *lane 1*). A similar immunoprecipitation experiment was performed with anti-SUMO-1 antibody, but no Rta bands were detected (Fig. 6*D*, *lanes 4–6*), because the anti-SUMO-1 antibody used in this study was unsuitable for immunoprecipitation (Zymed Laboratories Inc.).

Mapping Sumoylation Sites on Rta—Rta does not contain a conserved ψ*KX*E sequence, so several Rta deletion mutants were generated to investigate the sumoylation sites on Rta. A plasmid that expresses HA-Rta or its deletion derivatives was cotransfected with pCR-SUMO-1 into 293T cells. After the cells were cultured for 24 h, lysate was prepared and proteins in the lysate were immunoprecipitated and detected by immunoblotting with anti-HA antibody. The results revealed that the peptide fragment that contained the regions from amino acids 1 to 190 (RN190) and from 1 to 122 (RN122) of Rta was sumoylated (Fig. 7*A*). However, an Rta peptide fragment from amino acids 68 to 190 (R68/190) was not sumoylated (Fig. 7*A*), indicating that a sumoylation site is present between amino acids 1 and 67. Hence, the eight lysine residues in this region in RN190 were individually mutated. Changing the lysine residue at amino acid position 19 to alanine (RN190(K19A)) generated a peptide that could not be conjugated by SUMO-1 *in vivo* (Fig. 7*A*), indicating that Lys-19 is a sumoylation site. Therefore, a K19A mutation was generated in full-length Rta (Rta(19A)) to verify whether Lys-19 is a sumoylation site. Because SUMO-1 expressed from pCR-SUMO-1 contains a FLAG tag, this study used anti-FLAG antibody to immunoprecipitate SUMO-1-conjugated Rta from the lysate. Experimental results revealed that the K19A substitution did not influence the overall sumoylation pattern of Rta (Fig. 7*C*, *lane 3*). Furthermore, a deletion study also revealed that Lys-19 is not the only sumoylation site in Rta, because RN347, which contains the N-terminal 347 amino acids of Rta, was sumoylated even after K19A mutation (RN347(K19A)) (Fig. 7*A*), suggesting that the region between amino acids 191 and 347 of Rta may include additional sumoylation sites. Therefore, the lysine residues in this region in full-length Rta were individually mutated. An immunoprecipitation study revealed that a K213A substitution yielded a different pattern of Rta sumoylation (Fig. 7*C*, *lane 4*); not only with a lesser degree of overall Rta sumoylation but also without detectable 120- and 140-kDa Rta. The disappearance of these two bands could not be attributed to the insufficient loading of proteins to the gel (Fig. 7*B*, *lane 4*), because these two bands remained undetected even after overexposure of the blot to an x-ray film. Furthermore, although K19A mutation alone did not influence Rta sumoylation (Fig. 7*C*, *lane 3*), a double mutation of K19A and K213A, Rta(K19A/K213A), considerably

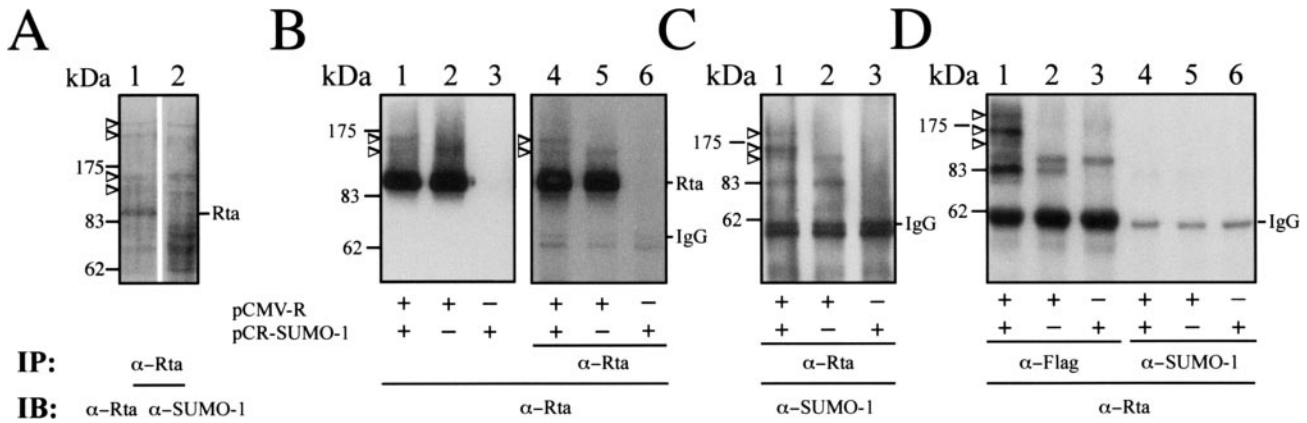

FIG. 6. **Detecting sumoylated Rta *in vivo*.** *A*, P3HR1 cells were treated with TSA to induce Rta expression. Rta and sumoylated Rta in cell lysate were immunoprecipitated (*IP*) with anti-Rta antibody and detected by immunoblot (*IB*) analysis with anti-Rta (*lane 1*) or anti-SUMO-1 antibody (*lane 2*). *B*, P3HR1 cells were transfected with pCMV-R (*lanes 2* and *5*), pCR-SUMO-1 (*lanes 3* and *6*), or cotransfected with both plasmids (*lanes 1* and *4*). Rta and sumoylated Rta in cell lysate were detected by immunoblot analysis with anti-Rta antibody (*lanes 1–3*) or immunoprecipitated and detected by immunoblot analysis with anti-Rta antibody (*lanes 4–6*). *C*, Rta and sumoylated Rta were immunoprecipitated with anti-Rta antibody and detected by immunoblotting with anti-SUMO-1 antibody. *D*, sumoylated Rta was immunoprecipitated with anti-FLAG antibody and detected with anti-Rta antibody (*lanes 1–3*) or immunoprecipitated with anti-SUMO-1 antibody and detected by anti-Rta antibody. Proteins were separated with 6% (*A*) or 8% (*B–D*) SDS-polyacrylamide gels. *Triangles* (*panel A*: 140 kDa, 160 kDa, 200 kDa, and 260 kDa; *panel B*: 140 kDa and 160 kDa; *panels C* and *D*: 140 kDa, 160 kDa, and 200 kDa) refer to sumoylated Rta.

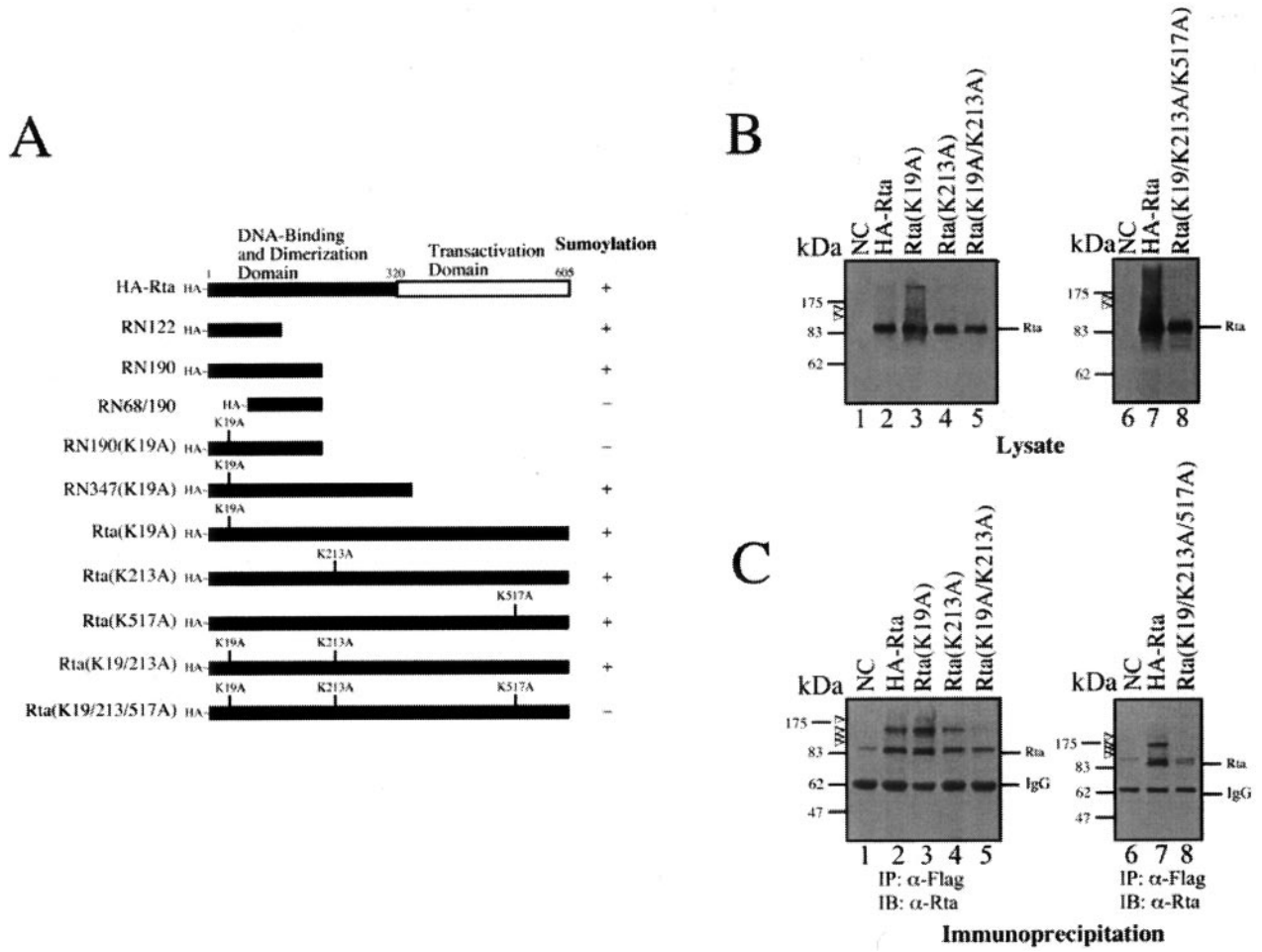

FIG. 7. **Mapping sumoylation sites on Rta.** HA-Rta was deleted to delineate the regions that contained a sumoylation site. Plasmids that expressed these proteins were cotransfected with pCR-SUMO-1 into 293T cells. Cells were lysed, and HA-tagged proteins were detected by immunoblot (*IB*) analysis with anti-HA antibody. K19A, K213A, and K517A indicate amino acid substitution by alanine at lysine residues 19, 213, and 517. The *numbers* in this *panel* specify the amino acid positions. *A*, the DNA binding and dimerization domains of Rta extend from amino acids 1 to 320; the transactivation domain was 321–605. Cells were also transfected with pCR-SUMO-1 and a plasmid that express full-length Rta containing a lysine to alanine substitution at the sumoylation sites. *B*, Rta in the lysate was analyzed by immunoblotting with anti-Rta antibody or immunoprecipitated with anti-FLAG antibody and detected by immunoblotting with anti-Rta antibody (*C*). *Triangles* (*panel B*: 140 kDa and 160 kDa; *panel C*: 120 kDa, 140 kDa, 160 kDa, and 200 kDa) refer to sumoylated Rta. *NC*, negative control, cells transfected with pcDNA3-HA; *HA-Rta*, Rta fused with an HA tag; *Rta(K19A)*, HA-Rta containing a K19A mutation; *Rta(K213A)*, HA-Rta containing a K213A mutation; *Rta(K19A/K213A)*, HA-Rta containing K19A and K213A mutations; *Rta(K19A/K213A/K517A)*, HA-Rta containing K19A, Lys-213, and Lys-517 mutations.

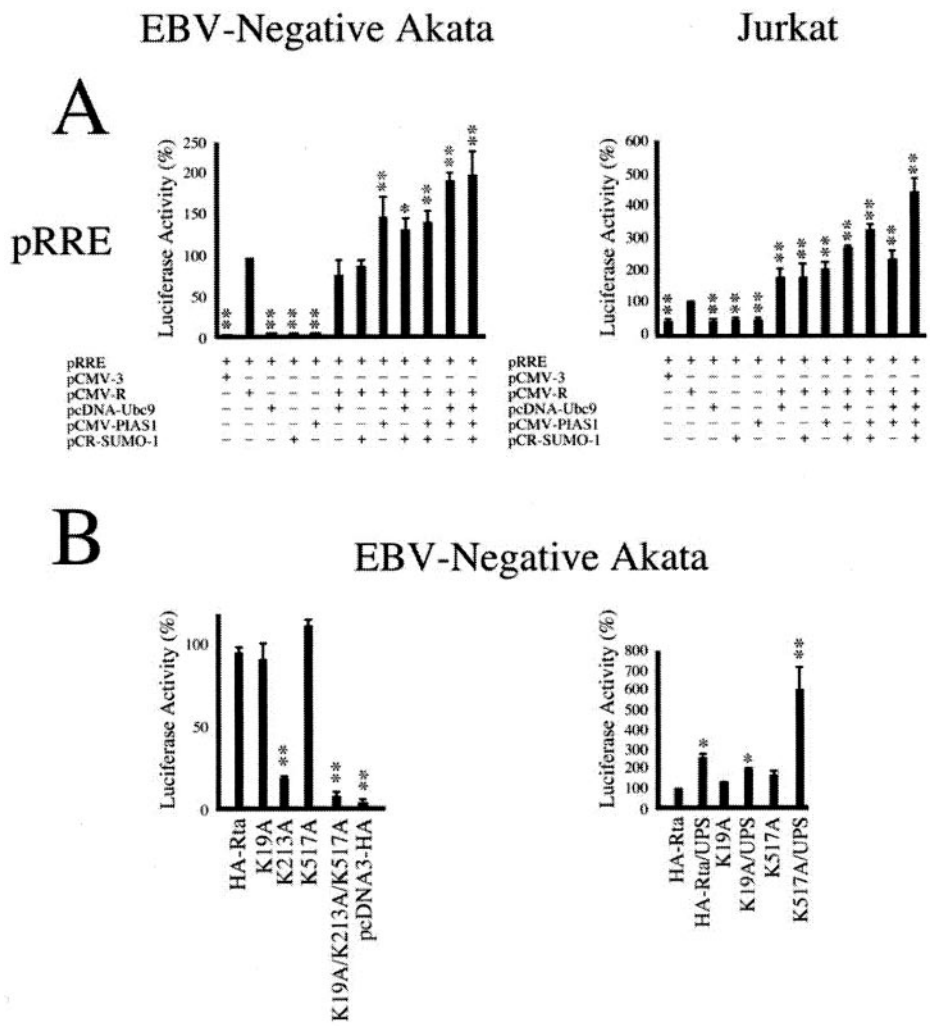

FIG. 8. **Enhancement of the transactivation activity of Rta by SUMO-1 conjugation.** *A*, EBV-negative Akata and Jurkat cells were cotransfected with pCR-SUMO-1, pCMV-PIAS1, and pcDNA-Ubc9, or with combinations of these plasmids, to elucidate the effects of the expression of Ubc9, PIAS1, and SUMO-1 on the capacity of Rta to transactivate an RRE promoter in pRRE. *B*, the effect of K19A, K213A, and K19A/K213A/K517A mutations of Rta to transactivated pRRE was investigated in EBV-negative Akata cells. A plasmid that expresses HA-tagged Rta, mutant Rta that contains a K19A mutation, a K213A mutation, a K517A mutation, or a K19A/K213A/K517A triple mutation, was cotransfected with pRRE. Cells were also cotransfected with plasmids that express Ubc9, PIAS1, and SUMO-1 (*UPS*) to examine how these proteins influence the transactivation activity. Luciferase activity exhibited by the cells was investigated at 24 h after transfection. Each transfection experiment was repeated at least twice, and each sample in the experiment was prepared in duplicate. Following a comparison with the value from the experiment involving pRRE/pCMV-R (*A*) or HA-Rta (*B*), the value from each experiment was analyzed statistically with the least square means method. *, $p < 0.05$; **, $p < 0.01$.

reduced Rta sumoylation (Fig. 7*C*, *lane 5*). The finding was reproducible, and the reduced sumoylation was not attributed to protein loading. However, these two substitutions did not completely eliminate Rta sumoylation as a trace amount of sumoylated HA-Rta at the position of 160 kDa remained detectable (Fig. 7*C*, *lane 5*), which became more evident when the blot was overexposed to an x-ray film (data not shown). Therefore, lysine residues were substituted into alanine in the C-terminal region in HA-Rta that had undergone K19A and K213A mutations. Finally, a third sumoylation site was identified at Lys-517; HA-Rta that contained a triple K19A, K213A, and K517A mutation was no longer sumoylated (Fig. 7*C*, *lane 8*).

Transient Transfection Analysis—In this work, a reporter plasmid, pRRE, which contains *luc* transcribed from a promoter that contains an Rta response element (RRE) from the BMLF1 promoter and a TATA sequence, was used to determine how Ubc9, PIAS1, and SUMO-1 affect the capacity of Rta to transactivate the RRE promoter. In EBV-negative Akata cells, the capacity of Rta to transactivate *luc* decreased slightly when Ubc9 or SUMO-1 was overexpressed in the cells (Fig. 8*A*). However, the overexpression of PIAS1 increased the transactivation ability of Rta to 155% (Fig. 8*A*). Moreover, the overexpression of two of the three sumoylation proteins increased the activity of Rta by 130–200% (Fig. 8*A*); Rta activity increased to 208% when Ubc9, PIAS1, and SUMO-1 were overexpressed in the cells (Fig. 8*A*). In Jurkat cells, transfecting a plasmid that expresses Ubc9, PIAS1, or SUMO-1 increased the ability of Rta to transactivate the *luc* gene in pRRE by ~200% (Fig. 8*A*). The presence of two of the three of these proteins increased Rta activity by around 230–320% (Fig. 8*A*). Rta activity increased to 440% when Ubc9, PIAS1, and SUMO-1 were overexpressed in the cell (Fig. 8*A*). In addition, EBV-negative Akata cells were also cotransfected with pRRE and pcDNA-HAR, which expressed HA-Rta. Although HA-Rta activated the RRE promoter in these cells (Fig. 8*B*), cotransfecting a plasmid (pcDNA-HAmR), which expresses the mutant Rta that contains triple K19A, K213A, and K517A substitutions, could not transactivate the expression of luciferase from the reporter plasmid (Fig. 8*B*); the luciferase activity exhibited by the reporter plasmid was at the background level. A transfection study revealed that K19A mutation slightly decreased but K517A mutation increased the transactivation activity of Rta by 168% (Fig. 8*B*). The K213A mutation, on the other hand, reduced the Rta transactivation activity approximately by 80% (Fig. 8*B*). Furthermore, cotransfecting plasmids that express Ubc9, PIAS1, and SUMO-1 enhanced the transactivation activity of Rta by 250% and Rta, which contains K19A mutation, by 199% (Fig. 8*B*). However, cotransfecting plasmids that express Ubc9, PIAS1, and SUMO-1 increased that ability of the Rta(K517) mutant to transactivate the RRE promoter by ~3-fold (Fig. 8*B*).

DISCUSSION

This investigation demonstrates that Ubc9 and PIAS1 bind to Rta both *in vitro* and *in vivo* (Figs. 1 and 3). Because Ubc9 and PIAS1 are involved in protein sumoylation (1, 54), the bindings suggest that Rta is modified by SUMO. Additionally, Rta con-

tains 605 amino acids and has an estimated molecular mass of 66 kDa. However, Rta normally migrates to positions significantly higher than 66 kDa in an SDS-polyacrylamide gel (52). To demonstrate that the 88-kDa band that we observed is Rta, this study analyzed the 88-kDa protein by MALDI-TOF mass spectrometry, which shows at least six peptide segments of this protein have a molecular mass consistent with that of the peptide segments of Rta, indicating that the 88-kDa protein is Rta. Furthermore, the mass increase of Rta to 88 kDa from 66 kDa cannot be attributed to phosphorylation, because unphosphorylated Rta migrates to the position slightly lower than 88 kDa at 85 kDa (55). Moreover, although SUMO-1 has an estimated molecular mass of ~12 kDa, earlier studies demonstrated that many SUMO-conjugated proteins, including Zta, Sp3, and IE72, usually have a size increase of ~20 kDa after conjugation by one SUMO-1 molecule (34, 37, 43). Although the 88-kDa protein is roughly 20 kDa larger than the estimated molecular mass of Rta, the increase in mass cannot be attributed to SUMO modification. This is because SUMO-conjugated proteins are typically unstable and rapidly hydrolyzed by SUMO-1 hydrolase during purification (19, 37). If this is also the case for SUMO-conjugated Rta, at least some 66-kDa Rta should have been detected by immunoblotting after purification. A failure to detect such a 66-kDa band by immunoblot analysis (Fig. 6) suggests that the 88-kDa Rta is not sumoylated.

Our conclusion indicating that Rta is conjugated by SUMO-1 comes from several results in this investigation. First, sumoylated Rta can be directly detected in lysate from P3HR1 cells activated for lytic replication (Fig. 6*A*). However, owing to the amount of Rta expressed after lytic induction being low, detection of sumoylated Rta becomes difficult and the bands representing sumoylated Rta are faint (Fig. 6*A*), explaining why this investigation transfected P3HR1 cells with plasmids that express Rta and SUMO-1 to increase the amount of Rta and SUMO-1 in the cells. Under such conditions, protein bands of 140 and 160 kDa were clearly detectable by immunoblot analysis with anti-Rta antibody (Fig. 6*B*, *lanes 1* and *2*), implying that Rta is modified by SUMO-1. Furthermore, these bands were extremely unstable and were undetected unless a lysis buffer containing SDS and NEM was used in the analysis, which also correlates with the characteristics of many SUMO-conjugated proteins (19, 37, 51). The evidence demonstrating that Rta is conjugated by SUMO-1 also comes from immunoprecipitation experiments. In the lysate prepared from P3HR1 cells transfected with a plasmid expressing Rta or cotransfected with plasmids expressing Rta and FLAG-tagged SUMO-1, sumoylated Rta was immunoprecipitated and detected by anti-Rta antibody (Fig. 6*B*, *lanes 4* and *5*) or anti-SUMO-1 antibody (Fig. 6*C*, *lanes 1* and *2*). Additionally, sumoylated Rta was immunoprecipitated by anti-FLAG antibody and detected by anti-Rta antibody (Fig. 6*D*, *lane 1*). Because the sumoylated Rta was undetected in the lysate prepared from the cells transfected only with pCMV-R (Fig. 6*D*, *lane 2*), this result eliminates the possibility that the proteins detected are nonspecifically immunoprecipitated by anti-FLAG antibody. Sumoylated Rta was also undetected in the lysate prepared from the cells transfected only with pCR-SUMO-1 (Fig. 6*D*, *lane 3*) (6), thus eliminating the possibility that the proteins detected are nonspecifically immunoprecipitated by anti-Rta antibody. This study also shows that sumoylated Rta is not immunoprecipitated by anti-SUMO-1 antibody (Fig. 6*D*, *lanes 4–6*). This is attributed to the fact that the antibody used in this study cannot be used for immunoprecipitation, which has also been reported in a previous study (51). Notably, the quantity of Rta that is sumoylated appears to be a small percentage of the total Rta (Fig. 6). This finding is unsurprising, because many studies have demonstrated that only a small fraction of the substrate, frequently below 1%, is sumoylated at any given time (56). Additionally, this investigation shows that cotransfecting a plasmid that expresses PIAS1 (Fig. 5*C*) or SUMO-1 (Fig. 6*B*) with pCMV-R increases not only the level of sumoylated Rta in the cell but also the activity of an RRE promoter in transient reporter assay (Fig. 8), showing that transactivation activity increases as more sumoyated Rta is detected.

This investigation demonstrates that PIAS1 is crucial in Rta sumoylation. Earlier studies suggested that SUMO E3 ligases, similar to ubiquitin E3, which contains a RING domain, do not possess intrinsic enzymatic activity but act as adaptors that bring together the E2 and the substrate (3, 18, 54). This work on Rta sumoylation and an earlier investigation by Johnson and Gupta (20) indicated that modifying a protein by SUMO-1 *in vitro* does not require PIAS1 (Fig. 5*A*). Rta sumoylation in the absence of PIAS1 probably results from the amounts of substrate and enzymes in the *in vitro* reactions being sufficient, which further explains why adding PIAS1 to the reactions was necessary for Rta sumoylation when the amounts of SUMO E1 and Ubc9 in the reaction mixtures were reduced (Fig. 5*B*). Additionally, in yeast two-hybrid screening, our results indicate that Rta binds to not only PIAS1, but also PIASXα and PIASXβ (data not shown), suggesting the importance of the interaction between Rta and SUMO E3 ligases in Rta sumoylation. Furthermore, a PIAS1 mutant that contains a C350S mutation in the RING domain (16) was not found to enhance the sumoylation of Rta *in vitro* (data not shown), indicating that PIAS1 is indeed critical for Rta sumoylation.

As is generally known, proteins are often sumoylated on the lysine residue of a ψKXE sequence. However, Rta does not contain such a sequence, even though two KXE sequences are present at amino acid positions 426 and 530. However, mutating the lysine residue of these two sites does not influence Rta sumoylation, indicating that these sequences are unrelated to Rta sumoylation. Rather, this investigation determines that Rta is sumoylated at Lys-19, Lys-213, and Lys-517. Other investigations have demonstrated that sumoylation at sites other than the lysine residue in a ψKXE sequence is reasonably common (57, 58). Additionally, proteins are frequently sumoylated at lysine residues that are preceded by a hydrophobic amino acid (8, 9). This finding seems also to apply to at least two of the three sumoylation sites in Rta, Lys-19 and Lys-517, which are preceded by Ile and Val, respectively. Unlike the other two lysine residues, the Lys-213 residue is not preceded by a hydrophobic amino acid. The structures of Rta in the Lys-213 region may provide an environment that permits the Lys-213 residue to be sumoylated. Furthermore, the conjugation of a protein by a SUMO-1 molecule usually increases molecular mass by 18–20 kDa (37), detecting 140-kDa sumoylated Rta by immunoprecipitation (Fig. 6*C*, *lane 1*; Fig. 6*D*, *lane 1*) is consistent with the notion that a single SUMO-1 molecule conjugates each of these three sumoylation sites. Additionally, detecting the 160- and 200-kDa bands (Fig. 6*C*, *lane 1* and Fig. 6*D*, *lane 1*) also suggests that Rta is polysumoylated, the finding of which is also supported by the fact that the 160-kDa sumoylated Rta remains detectable after both Lys-19 and Lys-213 are mutated (Fig. 7*C*, *lane 5*). Finally, the 160-kDa Rta may be more stable or abundant than the other sumoylated Rta molecules, because the band is normally more intense than the 140- or the 200-kDa band in immunoblots (Figs. 6 and 7).

According to our mapping study, mutating K19A alone does not seem to influence Rta sumoylation (Fig. 7*C*, *lane 3*). This phenomenon was frequently observed for proteins containing multiple sumoylation sites (36), possibly owing to the fact that each sumoylation site may be conjugated by various numbers of

SUMO molecules. Thus, eliminating only one sumoylation site may not completely alter the sumoylation pattern of the proteins. However, in contrast to Lys-19, mutating Lys-213 reduces Rta sumoylation (Fig. 7*C*, *lane 4*), implying that Rta is preferentially sumoylated at Lys-213.

Sumoylation often affects the function of a transcription factor (32). The transfection study demonstrates that overexpressing Ubc9, PIAS1, and SUMO-1 in EBV-negative Akata cells and Jurkat cells enhances the capacity of Rta to activate an RRE promoter (Fig. 8*A*). Among the three sumoylation sites in Rta, Lys-19 and Lys-213 are in the DNA binding domain of Rta. Although a K19A mutation does not influence the capacity of Rta to bind RRE, a mutant Rta with a K213A mutation does not bind to the element (data not shown), and so cannot activate an RRE promoter (Fig. 8*B*). This investigation also finds that, although the K19A mutation does not affect the activity of Rta, the Lys-517 mutation increases the transactivation activity of Rta 168% (Fig. 8*B*). Furthermore, overexpressing Ubc9, PIAS1, and SUMO-1 increases the activity of the Rta(K19A) mutant ~25% and the Rta(K517A) mutant by 3-fold (Fig. 8*B*), indicating that the sumoylation at Lys-19 is critical for the enhancing the transactivation activity of Rta.

As is generally known, transcription of BRLF1 and BZLF1 is undetectable by Northern blotting until 4 h after lytic induction (38), indicating that these two EBV immediate-early genes are expressed at low levels at the onset of the EBV lytic cycle. Despite the fact that Rta is expressed at a low level, Rta must autoregulate its own synthesis (59) and activate the expression of Zta (43), explaining why an EBV mutant defective in BRLF1 cannot efficiently complete the EBV lytic cycle (60). Therefore, an increase in transactivation activity of Rta by sumoylation (Fig. 3*A*) may be important for the early stage of EBV lytic development. Furthermore, Adamson and Kenney (43) demonstrated that Zta, is also sumoylated. These findings strongly suggest that sumoylation of both EBV immediate-early proteins is crucial to the lytic development of EBV.

Acknowledgments—We want to thank Frauke Melchior, Stefan Müller, and Van G. Wilson for providing the plasmids used in this study. We also thank Ming-Chieh Lin for his technical assistance.

REFERENCES

1. Melchior, F. (2000) *Annu. Rev. Cell Dev. Biol.* **16,** 591–626
2. Hay, R. T. (2001) *Trends Biochem. Sci.* **26,** 332–333
3. Hochstrasser, M. (2001) *Cell* **107,** 5–8
4. Kamitani, T., Kito, K., Nguyen, H. P., Fukuda-Kamitani, T., and Yeh, E. T. (1998) *J. Biol. Chem.* **273,** 11349–11353
5. Saitoh, H., and Hinchey, J. (2000) *J. Biol. Chem.* **275,** 6252–6258
6. Su, H., and Li, S. (2002) *Gene* (*Amst.*) **296,** 65–73
7. Mannen, H., Tseng, H. M., Cho, C. L., and Li, S. S. (1996) *Biochem. Biophys. Res. Commun.* **222,** 178–180
8. Rodriguez, M. S., Dargemont, C., and Hay, R. T. (2001) *J. Biol. Chem.* **276,** 12654–12659
9. Sampson, D. A., Wang, M., and Matunis, M. J. (2001) *J. Biol. Chem.* **276,** 21664–21669
10. Desterro, J. M., Rodriguez, M. S., Kemp, G. D., and Hay, R. T. (1999) *J. Biol. Chem.* **274,** 10618–10624
11. Okuma, T., Honda, R., Ichikawa, G., Tsumagari, N., and Yasuda, H. (1999) *Biochem. Biophys. Res. Commun.* **254,** 693–698
12. Desterro, J. M., Thomson, J., and Hay, R. T. (1997) *FEBS Lett.* **417,** 297–300
13. Gong, L., Kamitani, T., Fujise, K., Caskey, L. S., and Yeh, E. T. (1997) *J. Biol. Chem.* **272,** 28198–28201
14. Johnson, E. S., and Blobel, G. (1997) *J. Biol. Chem.* **272,** 26799–26802
15. Schwarz, S. E., Matuschewski, K., Liakopoulos, D., Scheffner, M., and Jentsch, S. (1998) *Proc. Natl. Acad. Sci. U. S. A.* **95,** 560–564
16. Kahyo, T., Nishida, T., and Yasuda, H. (2001) *Mol. Cell* **8,** 713–718
17. Pichler, A., Gast, A., Seeler, J. S., Dejean, A., and Melchior, F. (2002) *Cell* **108,** 109–120
18. Kagey, M. H., Melhuish, T. A., and Wotton, D. (2003) *Cell* **113,** 127–137
19. Kotaja, N., Karvonen, U., Janne, O. A., and Palvimo, J. J. (2002) *Mol. Cell. Biol.* **22,** 5222–5234
20. Johnson, E. S., and Gupta, A. A. (2001) *Cell* **106,** 735–744
21. Desterro, J. M., Rodriguez, M. S., and Hay, R. T. (1998) *Mol. Cell* **2,** 233–239
22. Muller, S., Matunis, M. J., and Dejean, A. (1998) *EMBO J.* **17,** 61–70
23. Lee, G. W., Melchior, F., Matunis, M. J., Mahajan, R., Tian, Q., and Anderson, P. (1998) *J. Biol. Chem.* **273,** 6503–6507
24. Zhang, H., Saitoh, H., and Matunis, M. J. (2002) *Mol. Cell. Biol.* **22,** 6498–6508
25. Zhong, S., Salomoni, P., Ronchetti, S., Guo, A., Ruggero, D., and Pandolfi, P. P. (2000) *J. Exp. Med.* **191,** 631–640
26. Sternsdorf, T., Jensen, K., and Will, H. (1997) *J. Cell Biol.* **139,** 1621–1634
27. Li, H., Leo, C., Zhu, J., Wu, X., O'Neil, J., Park, E. J., and Chen, J. D. (2000) *Mol. Cell. Biol.* **20,** 1784–1796
28. Zhong, S., Muller, S., Ronchetti, S., Freemont, P. S., Dejean, A., and Pandolfi, P. P. (2000) *Blood* **95,** 2748–2752
29. Goodson, M. L., Hong, Y., Rogers, R., Matunis, M. J., Park-Sarge, O. K., and Sarge, K. D. (2001) *J. Biol. Chem.* **276,** 18513–18518
30. Hong, Y., Rogers, R., Matunis, M. J., Mayhew, C. N., Goodson, M. L., Park-Sarge, O. K., Sarge, K. D., and Goodson, M. (2001) *J. Biol. Chem.* **276,** 40263–40267
31. Gill, G. (2003) *Curr. Opin. Genet. Dev.* **13,** 108–113
32. Verger, A., Perdomo, J., and Crossley, M. (2003) *EMBO Rep.* **4,** 137–142
33. Ross, S., Best, J. L., Zon, L. I., and Gill, G. (2002) *Mol. Cell* **10,** 831–842
34. Sapetschnig, A., Rischitor, G., Braun, H., Doll, A., Schergaut, M., Melchior, F., and Suske, G. (2002) *EMBO J.* **21,** 5206–5215
35. Rangasamy, D., and Wilson, V. G. (2000) *J. Biol. Chem.* **275,** 30487–30495
36. Ahn, J. H., Xu, Y., Jang, W. J., Matunis, M. J., and Hayward, G. S. (2001) *J. Virol.* **75,** 3859–3872
37. Spengler, M. L., Kurapatwinski, K., Black, A. R., and Azizkhan-Clifford, J. (2002) *J. Virol.* **76,** 2990–2996
38. Chang, L. K., and Liu, S. T. (2000) *Nucleic Acids Res.* **28,** 3918–3925
39. Chang, P. J., Chang, Y. S., and Liu, S. T. (1998) *J. Virol.* **72,** 5128–5136
40. Biggin, M., Bodescot, M., Perricaudet, M., and Farrell, P. (1987) *J. Virol.* **61,** 3120–3132
41. Flemington, E. K., Goldfeld, A. E., and Speck, S. H. (1991) *J. Virol.* **65,** 7073–7077
42. Takada, K., and Ono, Y. (1989) *J. Virol.* **63,** 445–449
43. Adamson, A. L., and Kenney, S. (2001) *J. Virol.* **75,** 2388–2399
44. Lin, J., Johannsen, E., Robertson, E., and Kieff, E. (2002) *J. Virol.* **76,** 232–242
45. Rosendorff, A., Illanes, D., David, G., Lin, J., Kieff, E., and Johannsen, E. (2004) *J. Virol.* **78,** 367–377
46. Luka, J., Kallin, B., and Klein, G. (1979) *Virology* **94,** 228–231
47. Davies, A. H., Grand, R. J., Evans, F. J., and Rickinson, A. B. (1991) *J. Virol.* **65,** 6838–6844
48. Schmidt, D., and Muller, S. (2002) *Proc. Natl. Acad. Sci. U. S. A.* **99,** 2872–2877
49. Ho, S. N., Hunt, H. D., Horton, R. M., Pullen, J. K., and Pease, L. R. (1989) *Gene* **77,** 51–59
50. Sambrook, J., Fritsch, E. F., and Maniatis, T. (1989) *Molecular Cloning: a Laboratory Manual*, 2nd Ed., Cold Spring Harbor Laboratory, Cold Spring Harbor, NY
51. Hofmann, H., Floss, S., and Stamminger, T. (2000) *J. Virol.* **74,** 2510–2524
52. Ragoczy, T., Heston, L., and Miller, G. (1998) *J. Virol.* **72,** 7978–7984
53. Gostissa, M., Hengstermann, A., Fogal, V., Sandy, P., Schwarz, S. E., Scheffner, M., and Del Sal, G. (1999) *EMBO J.* **18,** 6462–6471
54. Jackson, P. K. (2001) *Genes Dev.* **15,** 3053–3058
55. Zacny, V. L., Wilson, J., and Pagano, J. S. (1998) *J. Virol.* **72,** 8043–8051
56. Johnson, E. S. (2004) *Annu. Rev. Biochem.* **73,** 355–382
57. Lee, P. S., Chang, C., Liu, D., and Derynck, R. (2003) *J. Biol. Chem.* **278,** 27853–27863
58. Yamamoto, H., Ihara, M., Matsuura, Y., and Kikuchi, A. (2003) *EMBO J.* **22,** 2047–2059
59. Ragoczy, T., and Miller, G. (2001) *J. Virol.* **75,** 5240–5251
60. Feederle, R., Kost, M., Baumann, M., Janz, A., Drouet, E., Hammerschmidt, W., and Delecluse, H. J. (2000) *EMBO J.* **19,** 3080–3089
61. Muller, S., and Dejean, A. (1999) *J. Virol.* **73,** 5137–5143
62. Xu, Y., Ahn, J. H., Cheng, M., apRhys, C. M., Chiou, C. J., Zong, J., Matunis, M. J., and Hayward, G. S. (2001) *J. Virol.* **75,** 10683–10695